NISTIR 7738

Automated Extraction of Cellular Features for a Potentially Robust Classification Scheme

Shwetadwip Chowdhury

August 2010

National Institute of Standards and Technology
Technology Administration, U.S. Department of Commerce

NISTIR 7738

Automated Extraction of Cellular Features for a Potentially Robust Classification Scheme

Shwetadwip Chowdhury [1, 2]
[1] Information Technology Laboratory
[2] Duke University

August 2010

U.S. Department of Commerce
Gary Locke, Secretary

National Institute of Standards and Technology
Patrick D. Gallagher, Director

Abstract

The advent of new imaging technologies has allowed faster and higher-resolution cellular image acquisition by light microscopy. This has directly aided clinical research by allowing doctors and other researchers to better visualize cells and cellular components, which improves their ability to provide accurate prognosis, diagnosis, and treatment of a variety of diseases. However, a major bottleneck now is the manual evaluation of such images. Especially with the sheer amount of data being generated from these images, manual evaluation and analysis is becoming increasingly cumbersome. To address this concern, there has been extensive work on researching methods to automatically extract cellular and subcellular features that give morphological and functional insight into the cell. Some examples include extracting size/shape of cell boundaries, density of mitochondria, expression level of proteins, nuclear/cell size ratio, etc.

Here, we specifically focus on techniques to robustly extract information about the cellular proteins - actin, myosin, and phosphotyrosine - from images of cells specifically labeled with fluorescent moieties localized to the specific proteins. These proteins are known to be important components in the signaling pathways regulating cellular proliferation. Being able to quickly and automatically extract information about such proteins from raw images will greatly aid biological research, especially on topics related to understanding the role of the microenvironment in disease. Such extracted features can then be used for cellular classification. Future work can incorporate our feature extraction capabilities to classify a cell into categories with known feature parameters.

Acknowledgements

I would like to thank my advisor, Afzal Godil of NIST, for his guidance and support throughout this project. I would also like to thank Antonio Cardone of NIST, for his expertise on many relevant image processing topics as well as Kiran Bhadriraju of NIST for providing biomedical guidance, support, and direction to this project. Finally, I would like to acknowledge NIST's Summer Undergraduate Research Fellowship (SURF), which provided the funding and support for me to work on the project.

Introduction

Importance and Project Aim

In the past few decades, biomedical research has revolutionized healthcare by addressing many issues posed by limitations in medical knowledge or technology. Throughout its growth, however, much emphasis has still been placed on the ability to generate and analyze quantitative/visual information from a biological system. In such pursuits, medical imaging science has rapidly developed and, especially with dynamic and in-vivo organ/tissue systems, given birth to imaging techniques such as microscopy, Magnetic Resonance Imaging (MRI), ultrasound, and nuclear medicine which are now crucial in many modern diagnostic and prognostic procedures.

However, as medical imaging technology develops, allowing faster and higher-resolution image acquisition, acquisition speeds are steadily surpassing the rate at which experts can feasibly do accurate analysis. As such, a major bottleneck in the course from image acquisition to disease diagnosis is leaning increasingly towards image interpretation. This leads directly to a need for an automated image analysis ability that can keep up with the speeds of modern medical data generation techniques.

Generalized automated image analysis has received much attention from computer vision research, and many techniques developed in that field are applicable for our use. In particular, we focus on feature-based methods for object recognition. Feature-based methods are quite popular in computer vision, and several methods to extract features and cluster objects based on similarity are available [1-4]. However, many of these algorithms extract features describing mainly the physical appearance of the corresponding object. In biomedical settings, however, such features may often be too superficial. Especially in work to recognize and classify cells, the physical shape of the cell is heavily influenced by the sample's preparation, medium, and other extrinsic factors and cannot be attributed solely to the cell's identity or its other intrinsic properties. In this work, we aim to provide and discuss a few features for automatic cellular classification that have direct biological relevance to the cell itself, which can later potentially allow for a more robust cellular classification ability. Also, because of their biological bearing, these features should be able to be easily communicated to and understood by medical experts.

Paper Outline

In this paper, we will begin by giving a brief background. Because of the biomedical setting of this work, some emphasis will be placed on discussing relevant topics that are routinely handled by the biologists, though not directly associated with the main feature descriptor portions of the project. We will then proceed to describe features that may be useful for classification and discuss their possible extraction methods. We will then go over the limitations of this work and discuss possible future directions.

Background

Microscopy
When attempting to visualize biological systems smaller than what can be seen with the unaided eye, microscopy becomes a popular imaging technique. Optical microscopy, which uses visible light and a setup of lenses to magnify images of the sample, has rapidly gained use in this regard since its introduction via the simple light microscope several years ago. With the invention of digital cameras and other optical detectors, the analog signal from the sample image's magnification can be converted into a digital form. From here, established techniques from computer vision and digital signal processing can be applied to gain deeper insight into the data as well as pave the way towards automated image analysis. Especially along with its speed, ability to extract spectral information, and a minimal requirement for sample preparation, optical microscopy is a preferred, and in many cases more appropriate, microscopic technique than its electron or scanning-probe microscopy counterparts for many situations.

Fluorescence microscopy is a widely popular optical imaging technique used to image biological samples such as tissues sections [5]. For this technique, the biologist prepares the sample by tagging proteins of interest with fluorescent markers. The fluorescence excitation source is exposed to the sample, and at each point, the emitted fluorescence from the markers is captured by a CCD detector. The resulting image is then processed for image interpretation after feature extraction.

Biologically Relevant Molecules: Actin, Myosin, Focal Adhesion
In this particular project, we focus on visualizing actin, myosin, and focal adhesion protein patterns, so we briefly describe their roles in cellular function below [6]:

Actin is a protein with a critical role in the makeup of the cell's cytoskeleton. Important cellular processes that actin takes part in include maintenance of cell shape and structure, cell motility, and cell division. They appear as long strands in the cell.

Myosin is a protein that also contributes to cell motility and has importance in muscle fiber cells as well as all other cell types in the body, where it interacts with actin to provide contractile force.

Focal adhesions are protein assemblies that link an individual cell to the extracellular matrix, which provides basic structure and organization to cells in tissues and organs. As such, focal adhesions are important in allowing inter-cell communications, which form the basis for biological synchrony and cooperation. Biologically, focal adhesions are expected to appear at the ends of actin strands.

Materials

Data
Cell images were taken by a fluorescence microscope and saved as 16-bit TIFF format gray scale (14-bit wide gray channel). Cells were fluorescently tagged for actin, myosin, and focal adhesions and before imaging. Cell body was also imaged using its natural intrinsic fluorescence at near infra-red excitation wavelengths. The final data set contained 60 cell objects, with each object having been

imaged for its individual tags and body. It is assumed that there was no cellular movement while imaging the different tags so that image registration is not an issue.

Tools

MATLAB[i,ii] was used for the image processing and feature extraction techniques applied to the cellular images. The computer used was a 4 Gb, 3.2 GHz Dell PC.

Methods

Methods Introduction

This work is a subset in an umbrella project, which ultimately aims to extract robust, localized, and biologically-grounded features from cellular images. The over-arching project is divided into two parts:

1. Segmentation of localized regions within individual cells based on characteristics of interest
2. Extraction of features from the localized regions of interest (ROIs) outputted from part (1) described above.

The work described throughout the rest of this paper seeks to explore possibilities for part (2), and results for part (1) are saved for a future paper. Because part (2) requires a ROI from which to extract features from, for the sake of explanation, we consider our ROI to be a whole individual cell and most of our extracted features are taken as cellular, NOT sub-cellular, descriptors. Of course, most of the techniques described later can be applied equally as easily to localized regions in cells.

Image Preprocessing Steps

1. Each TIF image had its image intensity histogram equalized, which converted the original image with any predominant gray-scale pixel-values into an image where the full range of gray-scale values were used relatively equally among its pixels. This has the effect of increasing the global contrast of the image.
2. Much of the background was cropped off so that the cropped image would contain pixels predominantly inside the cell
3. The image was converted to gray scale

Cell Segmentation

We first choose a ROI to conduct later feature extractions on. For preliminary results, we choose a whole individual cell to be our ROI and we seek to get an accurate boundary for it. To do so, we use

[i] Registered trademark of The Mathworks, Inc. 3 Apple Hill Drive Natick, MA 01760-2098.

[ii] Any mention of commercial products within this report is for information only; it does not imply recommendation or endorsement by NIST

Otsu's 2D segmentation method [7] with n = 3 levels. After completing Otsu, the background pixels will predominantly be grouped into class 0, while the cellular pixels will be classified into classes 1 and 2. We mask for pixels that were not grouped into class 0 (thus capturing cellular pixels). We then perform basic binary morphological operations to smooth out the boundaries of the binary mask. After this processing, drawing the boundary on this binary image is a simple problem. From this boundary, typical features such as area, perimeter, and principal axes can be easily extracted. We find that the boundary extraction process works relatively well on various cellular images. Especially because this is to obtain only preliminary ROIs, this process is satisfactory for our goal. This process is graphically traced in Figure 1 below:

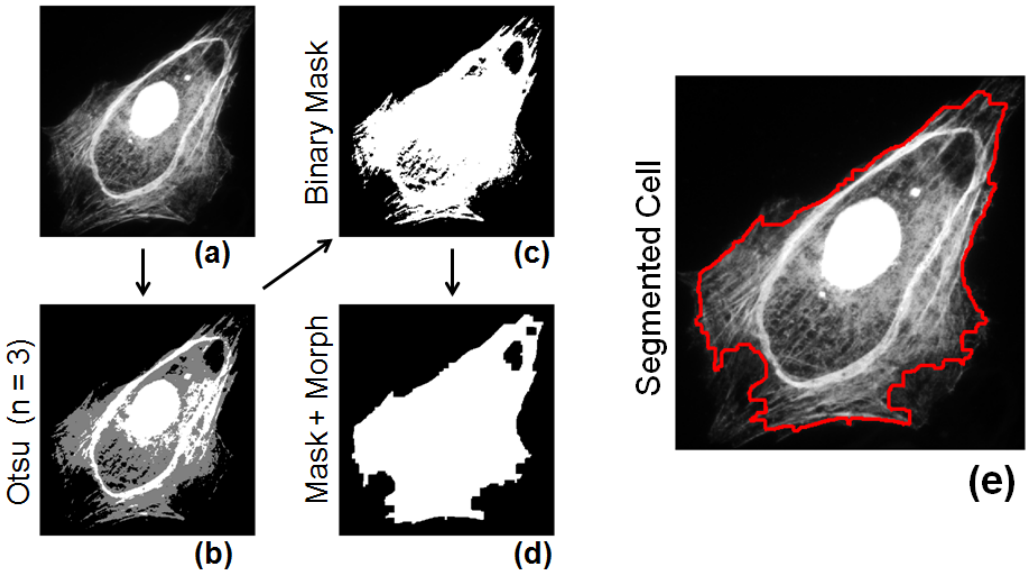

Figure 1 We start off with a raw image of the cell body (a). We run Otsu algorithm (n=3) to group the pixel intensities into 3 classes, where the background pixels fall mostly into one class, shown in black in (b). We mask for all non-background pixels (1c) and smooth out edges using standard morphological operations (1d). The border extracted from (1d) is shown superimposed on the original raw image of the cell body in (1e). Again, we stress that this border is used just to obtain a preliminary ROI to work further with. In the future, this ROI will often divided into smaller ROIs for more localized analysis.

Nuclear Segmentation

Extracting the cell nucleus boundary is an interesting extension to extracting the cell body boundary. It is medically known that many diseases and afflictions physically manifest in an abnormal nucleus/cell-body size ratio. Being able to accurately detect this ratio would give medical experts some power to detect for these afflictions. As explained above, we can compute a cell's area relatively accurately from its extracted boundary. We now seek to extract the cell nucleus's boundary, which will allow us to directly compute nucleus area. Furthermore, because nuclei are guaranteed to be well separated, extracting nuclei boundary would be a more robust method for counting the number of cells

in an image than extracting cell boundaries. The process described below details the procedure for nuclei extraction and Figure 2 provides an illustrative outline.

1. We start with an image of the cell that illuminates the nuclei well. For our purposes, we choose to start with the image showing the cellular focal adhesion fluorescent tags.
2. We blur the image. The purpose of this is to preserve mean intensities of significant portions of the cells while disregarding localized intensity spikes or dips that could result from segregate proteins or random signal variation. A typical blur kernel is an 11x11 array of ones.
3. We raise each image pixel intensity value to its 4^{th} power. Because the nuclei pixels will have higher average intensity from the rest of the cell, this will accentuate the intensity difference between the nucleus and the rest of the cell.
4. We convolve the image from step 3 with a 2D Gaussian profile. The resulting convolution will have maxima corresponding roughly to the centers of the nuclei. This allows us to locate centers of nuclei. Some maxima may have to be thresholded to account for localized intensity spikes in the original image not eliminated by the blurring in step 2.
5. We threshold the image from step 3. Because the nuclei have been accentuated from the rest of the cell, the threshold value should robustly work across many similar images. This step should output a mask that clearly shows the nuclei, though it may perhaps show some other disconnected and subsidiary structures from the original image.
6. From the nuclei centers computed from step 4, we flood fill to extract only the portions of the mask that are "connected" to nuclei-center pixels. This will output a binary mask containing only the nuclei.
7. Extract the boundary from the binary mask from step 6. Nuclear features like size, principle axis, etc can be easily extracted

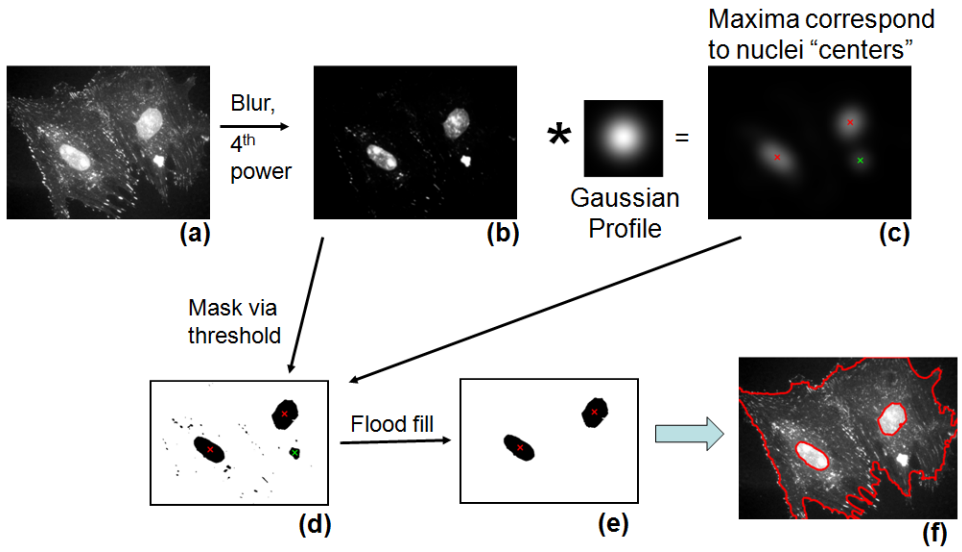

Figure 2 We start with the focal-adhesion image of two cells (a). Blurring the image and raising each pixel intensity to the 4^{th} power distinguishes the nuclei from surroundings (b), and centers are located by convolving with a Gaussian profile (c). Figure (b) is thresholded (d) and a flood-fill is carried out from the located nuclei centers, yielding a mask for the nuclei (e). Note that the maxima marked with a green X from (c) is thresholded out. Also note that the cell boundary locates only one "cell" while there are actually two cells in close proximity (f). Hence, number of nuclei boundaries is a more robust way of counting cells in an image.

Inter-Protein Correlation

Proteins are tailored for highly specific and tightly-controlled functions within a cell. As such, each protein's shape, location, and affinity for other proteins is at least partly determined by its function. Using fluorescent microscopy, protein location can be directly targeted, and a high correlation between cellular locations of two distinct proteins can imply, at least roughly, a similarity or association in function. In terms of image analysis, a simple pixel-by-pixel intensity correlation between fluorescent stains of the proteins in question will provide this metric and can be a useful feature.

We show below the correlation between actin/myosin and actin/focal adhesion (FA) images of a sample cell. Biologically, actin and myosin have associated functions and appear in similar cell locations. On the other hand, FAs link cells to the extracellular matrix and therefore their correlation with actin is not expected to be as high as actin/myosin correlation. Figure 3 below shows this.

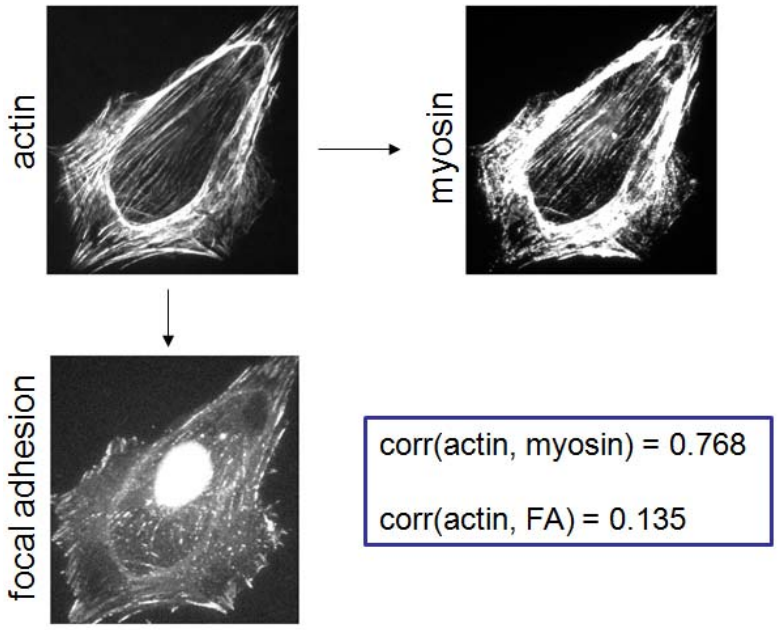

Figure 3 Myosin and actin are biologically known to have associated functions. As expected, the correlation between actin and myosin shown above is much higher than between actin and FA.

Bulk Texture

Another common metric used to describe an ROI is its texture features. Intuitively, these features describe properties such as image smoothness, roughness, homogeneity, etc. Statistical texture features are calculated from the image histogram, and they provide bulk measures for the image with no directional information. These features are well established [8] and are listed below.

Mean	$m = \sum_{i=0}^{L-1} z_i \, p(z_i)$
Standard Deviation	$\sigma = \sum_{i=0}^{L-1} (z_i - m)^2 \, p(z_i)$
Smoothness	$R = 1 - \frac{1}{1+\sigma^2}$
Third moment	$\mu_3 = \sum_{i=0}^{L-1} (z_i - m)^3 \, p(z_i)$
Uniformity	$U = \sum_{i=0}^{L-1} p^2(z_i)$
Entropy	$e = -\sum_{i=0}^{L-1} p(z_i) \log_2 p(z_i)$

Table 1 Bulk texture features calculated from the image histogram. L is the number of pixel intensities in the image. z_i is the number of pixels with intensity i. $p(z_i)$ is the probability that an image pixel has intensity i.

Directional Texture

Bulk texture values calculated from the image histogram do not contain any information about relative orientations of pixels. Some proteins, particularly actin, occur in highly directional patterns. In situations like these, bulk texture features will not capture many specific properties, and a texture-analysis procedure that considers distribution of intensities as well as relative positions of pixels is needed.

A popular method [9] to do this uses a co-occurrence matrix to calculate directional texture values. For an image with L pixel intensities, ranging from 0 to Z_{L-1}, co-occurrence matrix M is of size LxL. The entry at position (i,j) in the matrix is the number of times that image pixel pairs at a user-specified offset occur simultaneously with intensity Z_i and Z_j. Different co-occurrence matrices will be calculated for different offsets. Mathematically, the matrix for image I of size X by Y pixels can be written as:

$$M_{(\Delta x,\Delta y)}(i,j) = \sum_{m}^{X}\sum_{n}^{Y} \begin{cases} 1 & if\ I(m,n) = i\ and\ I(m+\Delta x, n+\Delta y) = j \\ 0 & else \end{cases}$$

where $M_{(\Delta x,\Delta y)}$ is the particular co-occurrence matrix at the offset specified by $(\Delta x, \Delta y)$. From the co-occurrence matrix, texture features along the offset can be found:

Contrast	$\sum_{i,j} \lvert i-j \rvert^2 p(i,j)$
Correlation	$\sum_{i,j} \frac{(i-\mu i)(j-\mu j)p(i,j)}{\sigma_i \sigma_j}$
Uniformity	$\sum_{i,j} p(i,j)^2$
Homogeneity	$\sum_{i,j} \frac{p(i,j)}{1+\lvert i-j \rvert}$

Table 2 Equations to calculate directional texture features from co-occurrence matrix

where *(i,j)* iterate through the co-occurrence matrix and

$$p(i,j) = \frac{M(i,j)}{\sum_{m,n} M(m,n)}$$

Extracting Orientations and Coherence

With cells containing highly directional information, it is useful to extract features that describe prominent orientations. Particularly in terms of this work, extraction and analysis of the orientations of cellular actin fibers can allow study into cytoskeleton structure, cell phase, cell motility, etc. We briefly describe an approach for extracting image orientations proposed in [10] that is based on taking pixel-by-pixel intensity gradients from the image.

We define gradient vector $\boldsymbol{G} = \langle G_x, G_y \rangle$ at each position in image *I*, such that:

$$\begin{bmatrix} G_x(x,y) \\ G_y(x,y) \end{bmatrix} = \begin{bmatrix} \frac{\delta}{\delta x} I(x,y) \\ \frac{\delta}{\delta y} I(x,y) \end{bmatrix}$$

For each location in *I*, we use a surrounding region *W* (often a weighted Gaussian region) to compute vector $\widehat{\boldsymbol{G_s}} = \langle G_{xx} - G_{yy}, 2\, G_{xy} \rangle$ such that:

$$G_{xx} = \sum\nolimits_W G_x^2 \qquad G_{yy} = \sum\nolimits_W G_y^2 \qquad G_{xy} = \sum\nolimits_W G_x G_y$$

It is shown in [10] that orientation (θ) is robustly computed at the pixel level by:

$$\theta = \begin{cases} \phi + \frac{1}{2}\pi & \phi \leq 0 \\ \phi - \frac{1}{2}\pi & \phi \geq 0 \end{cases} \qquad \text{where} \qquad \phi = \frac{1}{2} \angle \widehat{\boldsymbol{G_s}}$$

The coherence *Coh*, a metric for how unidirectional orientations are in localized area *W*, is also included in [10]:

$$Coh = \frac{|\sum_W \widehat{\boldsymbol{G_s}}|}{\sum_W |\widehat{\boldsymbol{G_s}}|}$$

In our case, when applied to images of cellular actin, $\theta(x, y)$ and $Coh(x, y)$ gives the orientation and directional uniformity respectively of actin fibers at each point *(x,y)* in image *I*. We construct a histogram of oriented gradients (HOG) directly from $\theta(x, y)$, which allows analysis of features such as predominant actin directions and uniformity of actin directions directly from typical histogram descriptors. We show an example of calculated orientations, coherence, and HOG in Figure 4 below:

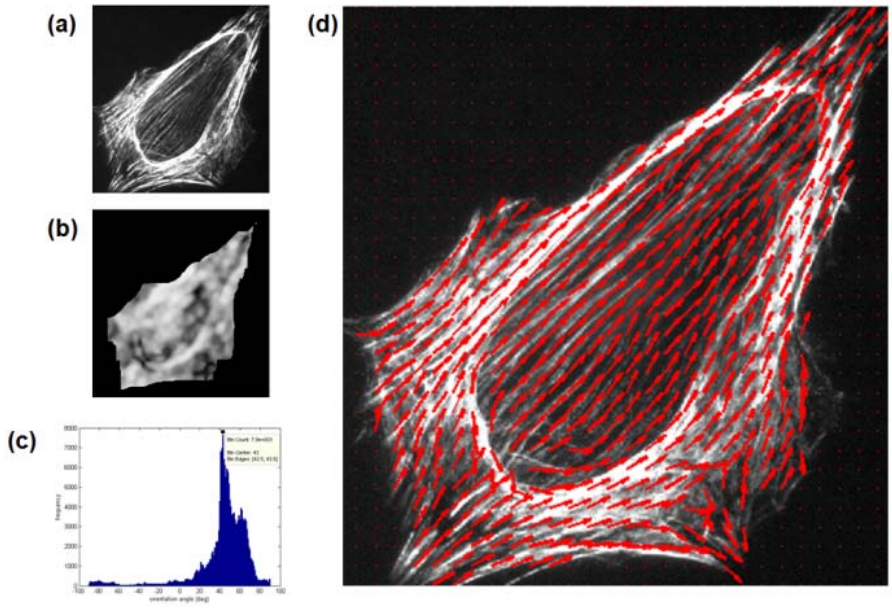

Figure 4 Raw image of cellular actin (a) is processed to extract the coherence (b) and histogram of oriented gradients (c) from the pixel by pixel orientations (d).

There has been work done to distinguish regions of a cell based on differences in orientation of actin fiber. A potential scheme to do this can be based on segmenting between regions with significant actin orientation differences. Features that can directly be extracted from this can include average sizes of regions with relative actin uniformity, number and locations of such regions, etc. Figure 5 below shows an example relating to this method:

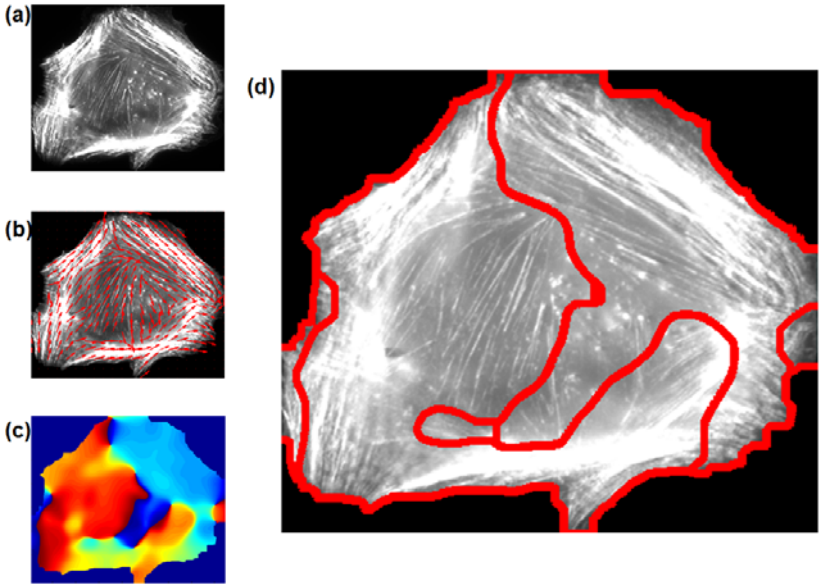

Figure 5 Raw image of cellular actin (a) is processed to extract the orientations (b). The orientations are then segmented based on significant value changes (c) to extract borders bounding regions of relative uniform

Importance of Extracting Actin

As explained before, actin is an important biomolecule responsible for making up the cytoskeleton and critical for cell movement. To a specialized biologist, it may be important to have access to features describing the actin at single-fiber level. For such cases, it is imperative that actin can be robustly extracted from surroundings, which will in turn improve the accuracy of extracted actin features described later.

We present below a preliminary actin extraction scheme. However, we stress that this extraction scheme needs further development before public use.

Potential Actin Extraction Scheme

The actin extraction procedure used for this work has been adapted from [11] and we outline it below.

Extraction Procedure

1. Define fiberscore image to be $I_{fb}(x, y)$ to be same size as input image $I(x, y)$. Initialize I_{fb} to contain only zeros
2. Define a kernel $K(\theta)$ to be a sparse array of size $(2l + 1) \times (2l + 1)$ with ones through the center at angle θ
3. Iterate θ_m from 0 → $\frac{\pi}{2}$
4. For each iteration, define kernels $K(\theta_m)$ and $K(\theta_m + \frac{\pi}{2})$
5. For each location (i, j) in image $I(x, y)$
    a. Define image subregion I_r of size $(2l + 1) \times (2l + 1)$ so that $I_r(x, y) = I(i - l + x - 1, j - l + y - 1)$
    b. Define $L_{i,j}(\theta_m)$ to be a vector containing nonzero elements of the element-by-element product of $I_r(x, y)$ and $K(\theta_m)$. Define $L_{i,j}(\theta_m + \frac{\pi}{2})$ to be the corresponding vector for $I_r(x, y)$ and $K(\theta_m + \frac{\pi}{2})$.

c. From $L_{i,j}(\theta_m)$, compute mean, standard deviation, normalized standard deviation, and correlation to non-zero entries in $K(\theta_m)$. Denote these as $M_{i,j}(\theta_m)$, $SD_{i,j}(\theta_m)$, $NSD_{i,j}(\theta_m)$, $Corr_{i,j}(\theta_m)$, respectively. Define and compute corresponding values of $M_{i,j}\left(\theta_m+\frac{\pi}{2}\right)$, $SD_{i,j}\left(\theta_m+\frac{\pi}{2}\right)$, $NSD_{i,j}\left(\theta_m+\frac{\pi}{2}\right)$, $Corr_{i,j}\left(\theta_m+\frac{\pi}{2}\right)$ from $L_{i,j}\left(\theta_m+\frac{\pi}{2}\right)$ and $K(\theta_m+\frac{\pi}{2})$.

d. IF $M_{i,j}(\theta_m), NSD_{i,j}(\theta_m), NSD_{i,j}(\theta_m)/NSD_{i,j}(\theta_m+\pi/2)$, and $Corr_{i,j}(\theta_m)$ pass user-set thresholds
THEN $I_{fb}(i,j)=\max\left(Corr_{i,j}(\theta_m), I_{fb}(i,j)\right)$

e. ELSE IF $M_{i,j}(\theta_m+\pi/2), NSD_{i,j}(\theta_m+\pi/2), NSD_{i,j}(\theta_m+\pi/2)/NSD_{i,j}(\theta_m)$, and $Corr_{i,j}(\theta_m+\pi/2)$ pass user-set thresholds
THEN $I_{fb}(i,j)=\max\left(Corr_{i,j}\left(\theta_m+\frac{\pi}{2}\right), I_{fb}(i,j)\right)$

6. Repeat steps 4-5 with next iteration of θ_m
7. Output image $I_{out}(x,y)=$ OTSU$\left(I_{fb}(x,y),2\right)$ where function OTSU(I,n) performs the Otsu segmentation on image I with n levels

Figure 6 below shows actin extraction via this procedure:

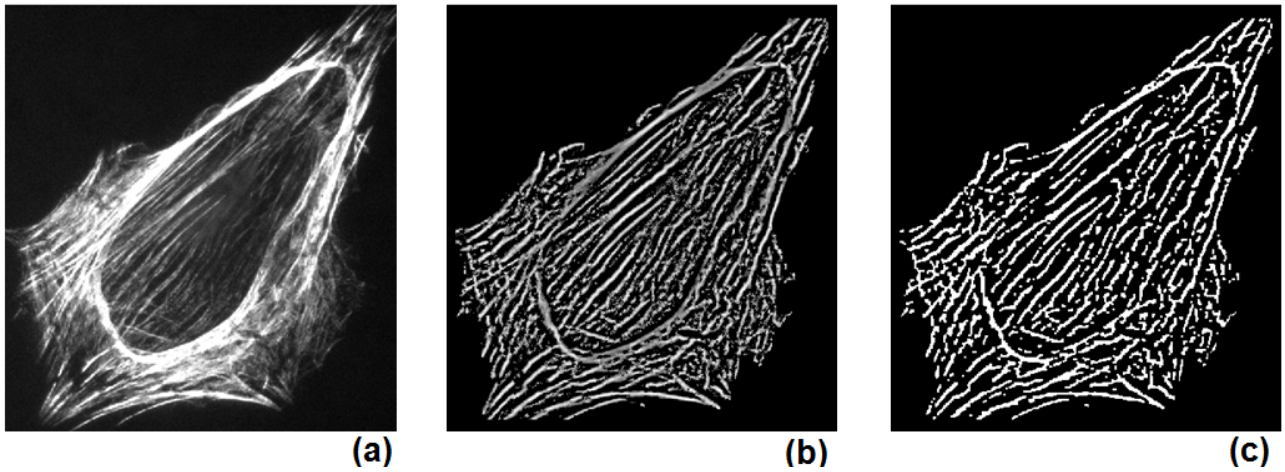

Figure 6 Raw image of cellular actin (a) is processed using the described procedure to extract a fiberscore image (b). The fiberscore image is thresholded to yield the final outputted image (c).

Actin Width and Density

After binarizing the cell with respect to its actin, it becomes a simple matter to calculate features describing actin widths and density.

By scanning horizontally across the binary image of actin, horizontal cuts of individual actin fibers (assumed to be connected white pixels) are directly extracted. By recalling that we also have orientation information, calculating actin cross-sectional width becomes simple trigonometry (Figure 7). Thus, we can construct a histogram of pixel-by-pixel cross sectional widths, and features describing actin mean-width and uniformity can be extracted.

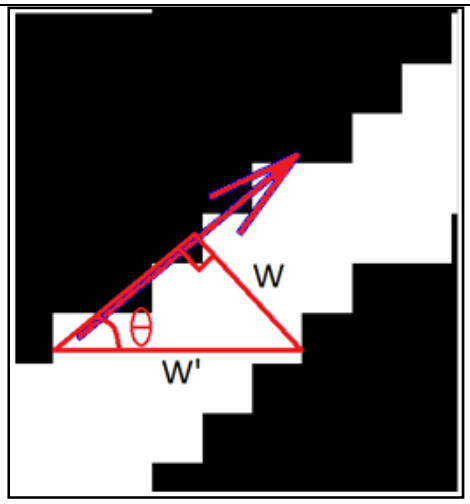

Figure 7 A close up of an actin fiber from Figure 6c is shown. Cross-sectional actin width W can be found by extracting a horizontal cut W' and using previously calculated orientation θ values to calculate $W = W' \sin(\theta)$

If we skeletonize the binary actin image, we reduce each actin fiber to single pixel widths. By doing so, actin density can be computed by simply taking the ratio of white (actin) pixels to total pixels in the skeletonized image. This computed density would have units of # actin fibers/pixel and can be used to estimate the number of actin fibers in a given region of known size. We note again that the accuracy of this computation as well as the widths-extraction mentioned above critically depends on the robustness of the actin extraction algorithm.

Concluding Remarks and Future Work

We have provided above a preliminary set of biological features that can be extracted with relative ease from cellular images, be easily communicated to biologists, and contribute to a more robust classification scheme. Though we have focused exclusively on very specific types of images, we hope that the methods presented here can be modified and extended to a wide range of cellular images. However, for this work in particular, there is still much room for growth, and we mention below a few potential features that could offer more biological and quantitative insight, as well as added power to the classification process.

1. Descriptors for the distribution of actin fiber lengths
2. Metric for how physically localized focal adhesion spots are to the ends of actin fibers
3. Descriptors for the relationship between localized inter-protein correlations and localized actin densities.
4. Descriptors for the relationship between localized inter-protein correlations and orientation coherence

References

1. B. Moghaddam and A. Pentland, "Probabilistic Visual Learning for Object Representation". IEEE Trans. Pattern Analysis and Machine Intelligence, vol 19, no. 7, pp 696-710, July 1997

2. Mark Lillholm, Mads Nielsen, Lewis Griffin, “Feature based Image Analysis” International Journal of Computer Vision, vol 52, issue 2-3, pp 73-95, 2003

3. Lowe, David G. (1999). "Object recognition from local scale-invariant features". Proceedings of the International Conference on Computer Vision. 2. pp. 1150–1157.

4. Herbert Bay, Andreas Ess, Tinne Tuytelaars, Luc Van Gool "SURF: Speeded Up Robust Features", Computer Vision and Image Understanding (CVIU), Vol. 110, No. 3, pp. 346--359, 2008

5. Fellers TJ, Davidson MW (2007). "Introduction to Confocal Microscopy". Olympus Fluoview Resource Center. National High Magnetic Field Laboratory.

6. Bruce Alberts, Alexander Johnson (1994) " Molecular Biology of the Cell", New York: Garland Publishing Inc

7. Nobuyuki Otsu (1979). "A threshold selection method from gray-level histograms". IEEE Trans. Sys., Man., Cyber. 9: 62–66

8. R. C. Gonzalez, R. E. Woods, & S. L. Eddins, Digital Image Processing Using MATLAB, Prentice-Hall, 2004

9. Robert M. Haralick, "Statistical and structural approaches to texture," Proc. IEEE, vol. 67, no. 5, pp. 786-804, 1979

10. A. M. Bazen and S. H. Gerez, "Systematic Methods for the Computation of the Directional Fields and Singular Points of Fingerprints," IEEE Trans. Pattern Analysis and Machine Intelligence, vol. 24, no. 7, pp 905-919, July 2002

11. N .Lichtenstein, B. Geiger, "Quantitative analysis of cytoskeletal organization by digital fluorescent microscopy",vol. 54A, issue 1, pp 8-18, Cytometry Part A. June 2003